

# Molecular, functional and structural properties of the prolyl oligopeptidase of *Trypanosoma cruzi* (POP Tc80), which is required for parasite entry into mammalian cells

Izabela M. D. BASTOS\*, Philippe GRELLIER†, Natalia F. MARTINS‡, Gloria CADAVID-RESTREPO\*, Marian R. DE SOUZA-AULT\*, Koen AUGUSTYNS§, Antonio R. L. TEIXEIRA\*, Joseph SCHRÉVEL†, Bernard MAIGRET||, José F. DA SILVEIRA¶ and Jaime M. SANTANA\*<sup>1</sup>

\*Laboratório Multidisciplinar de Pesquisa em Doença de Chagas (CP 04536), Universidade de Brasília, 70919-970, Brasília, DF, Brazil, †USM 0504, Département Régulations, Développement, Diversité Moléculaire, Muséum National d'Histoire Naturelle, 61 rue Buffon, 75231, Paris Cedex 05, France, ‡Embrapa, Genetic Resources and Biotechnology, CP 02372, Brasília, DF, Brazil, §Department of Medicinal Chemistry, The University of Antwerp, Belgium, ||Laboratoire de Chimie Théorique, Université de Nancy, 54506 Vandoeuvre-les-Nancy, France, and ¶Departamento de Microbiologia, Imunologia e Parasitologia, Escola Paulista de Medicina, R. Botucatu 862, CEP 04023-062, São Paulo, SP, Brazil

We have demonstrated that the 80 kDa POP Tc80 (prolyl oligopeptidase of *Trypanosoma cruzi*) is involved in the process of cell invasion, since specific inhibitors block parasite entry into non-phagocytic mammalian host cells. In contrast with other POPs, POP Tc80 is capable of hydrolysing large substrates, such as fibronectin and native collagen. In this study, we present the cloning of the *POPTc80* gene, whose deduced amino acid sequence shares considerable identity with other members of the POP family, mainly within its C-terminal portion that forms the catalytic domain. Southern-blot analysis indicated that *POPTc80* is present as a single copy in the genome of the parasite. These results are consistent with mapping of *POPTc80* to a single chromosome. The active recombinant protein (rPOP Tc80) displayed kinetic properties comparable with those of the native enzyme. Novel in-

hibitors were assayed with rPOP Tc80, and the most efficient ones presented values of inhibition coefficient  $K_i \leq 1.52$  nM. Infective parasites treated with these specific POP Tc80 inhibitors attached to the surface of mammalian host cells, but were incapable of infecting them. Structural modelling of POP Tc80, based on the crystallized porcine POP, suggested that POP Tc80 is composed of an  $\alpha/\beta$ -hydrolase domain containing the catalytic triad Ser<sup>548</sup>–Asp<sup>631</sup>–His<sup>667</sup> and a seven-bladed  $\beta$ -propeller non-catalytic domain. Docking analysis suggests that triple-helical collagen access to the catalytic site of POP Tc80 occurs in the vicinity of the interface between the two domains.

**Key words:** mammalian cell, prolyl oligopeptidase, structural modelling, Tc80 proteinase, *Trypanosoma cruzi*, trypomastigote.

## INTRODUCTION

Chagas disease, a chronic debilitating illness, is caused by the protozoan parasite *Trypanosoma cruzi*. Eighteen million people are estimated to be infected with *T. cruzi*, while millions are at risk of acquiring the infection in those areas where the disease is still endemic [1]. Distribution of *T. cruzi* throughout vertebrate host tissues depends on the ability of the parasite to cross basement membranes and the extracellular matrix to reach and invade host cells. An important step in this process is a specific interaction of the trypomastigote form of the parasite with collagens, laminin, fibronectin and heparin, that ensures parasite entry into host cells [2,3]. In agreement with these features of the *T. cruzi*–vertebrate host interaction, we have postulated that the parasite synthesizes an enzyme displaying collagenase activity that could facilitate parasite entry into host cells. Such a proteinase has been identified, purified and biochemically characterized as a secreted 80 kDa neutral enzyme (Tc80 proteinase) with activity on human type I and IV collagens and less extensively on fibronectin [4,5]. Moreover, we have demonstrated that the Tc80 proteinase also mediates native collagen type I hydrolysis with features comparable with those displayed by the *Clostridium histolyticum* col-

lagenase [4]. These biochemical and enzymatic properties of Tc80 have suggested that the protein could be involved in the infection process by facilitating parasite migration through the extracellular matrix and interaction with host cell-membrane components. Using specific inhibitors against Tc80 [6,7], we have performed preliminary studies on the protein's physiological role in the *T. cruzi*–mammalian host cell interaction [5]. Tc80 enzymatic activity is specifically inhibited by these molecules, precluding host cell infection by trypomastigotes in a dose-dependent manner. This demonstrated that the proteinase is indeed involved in a non-phagocytic mammalian cell invasion process by *T. cruzi*, and could be a potential target for chemotherapy of vertebrate *T. cruzi* infection.

In accordance with its inhibition pattern and high specificity for peptide bonds at the carboxyl end of proline residues, Tc80 has been considered to be a member of the POP (prolyl oligopeptidase; EC 3.4.21.26; also known as post-proline cleaving enzyme and prolyl endopeptidase) family (S9) of serine proteinases [8] and renamed as POP Tc80 (POP of *T. cruzi*) [5]. In addition to the so-called POP, this group of proteinases also includes oligopeptidase B, acylaminoacyl peptidase and dipeptidyl peptidase IV, because, in spite of low primary sequence similarity, these enzymes

Abbreviations used: AMC, 7-amido-4-methylcoumarin; Boc, t-butoxycarbonyl; Cbz, benzyloxycarbonyl; DAPI, 4,6-diamidino-2-phenylindole; DTT, dithiothreitol; FAP, fibroblast activation protein; IPTG, isopropylthio- $\beta$ -D-galactoside; ORF, open reading frame; POP, prolyl oligopeptidase; POP Tc80, POP of *Trypanosoma cruzi*; rPOP Tc80, recombinant POP Tc80; UTR, untranslated region.

<sup>1</sup> To whom correspondence should be addressed (email jsantana@unb.br).

The nucleotide sequence data reported have been submitted to the DDBJ, EMBL, GenBank® and GSDB Nucleotide Sequence Databases under the accession number AF452421.

share a similar three-dimensional structure and have been considered as members of the  $\alpha/\beta$ -hydrolase fold enzyme family. The structure of porcine POP shows a cylindrical shape consisting of a peptidase domain and a seven-bladed  $\beta$ -propeller domain [9]. It has been proposed that the most distinguishing peculiarity of the POP family members is their specificity for oligopeptides not longer than 30 amino acid residues because the  $\beta$ -propeller domain would exclude larger substrates from the enzyme active site [9]. However, we found that the purified POP Tc80 hydrolyses large protein substrates such as collagens and fibronectin as well as small peptides [4,5].

The aim of the present study was to characterize the *POPTc80* gene, to express the proteinase in a heterologous system and compare its kinetic properties with those of its native form and to obtain information about its three-dimensional structure. We also established the role of POP Tc80 in parasite invasion of mammalian cells by the employment of specific inhibitors.

## EXPERIMENTAL

### Parasites

*T. cruzi* epimastigote forms from Tulahuén stock were grown in liver infusion tryptose medium supplemented with 100 units/ml penicillin, 100  $\mu$ g/ml streptomycin and 10% (v/v) fetal calf serum at 28°C with continuous agitation. Trypomastigotes and amastigotes of the parasite were obtained by monolayer culture of murine muscle L-6 cells grown in RPMI medium containing 10% fetal calf serum at 37°C in 5% CO<sub>2</sub> and then purified as described previously [10,11].

### Isolation of the *POPTc80* gene

Reverse primers containing 3'-UTR (3'-untranslated region; *pop-utr*, 5'-CGCAACATTCTTTCCACACGTTCC-3') and stop codon (*pop-nested*, 5'-GCAGTCCACCTTATTACTCTTTCC-3') were designed from a *T. cruzi* expressed sequenced tag (EMBL accession no. AW325010) clone, whose deduced amino acid sequence matched perfectly with two internal tryptic peptides from purified POP Tc80 [5]. The *pop-utr* primer was used to synthesize first-strand cDNA from 5  $\mu$ g of total epimastigote RNA (extracted with TRIzol<sup>®</sup> reagent; Gibco BRL, Gaithersburg, MD, U.S.A.) using the SUPERScript<sup>™</sup> kit (Gibco BRL) according to the manufacturer's instructions. The complete *POPTc80* sequence was obtained by PCR using 1  $\mu$ l (5%) of epimastigote cDNA reaction mixture combined with miniexon forward primer (5'-TTGCTACAGTTTCTGTACTATATT-3'; [12]) and *pop-nested* as described above. PCR was performed as follows: 94°C for 2 min followed by 30 cycles at 94°C for 30 s, 55°C for 30 s and 72°C for 3 min with a final extension of 10 min at 72°C. The 2176 bp product was directly cloned into pCR4-TOPO<sup>®</sup> (Invitrogen, Carlsbad, CA, U.S.A.), generating TOPO-*POPTc80*, which was completely sequenced in both directions to confirm its authenticity. The POP Tc80 cDNA sequence is available in GenBank<sup>®</sup> database under accession no. AF452421.

### Genomic organization of POP Tc80

DNA of *T. cruzi* was purified according to the method of Medina-Acosta and Cross [13]. The *POPTc80* gene molecular karyotype was performed by Southern blotting of the *T. cruzi* chromosome separated by pulsed-field gel electrophoresis [14]. To evaluate the number of *POPTc80* genomic copies, 5  $\mu$ g aliquots of *T. cruzi* genomic DNA were digested with BamHI, ClaI, EcoRV, HindIII and XhoI restriction enzymes for 16 h, electrophoretically

separated on 0.8% agarose gels and blotted on to nylon membrane. The membranes were probed with random-primed <sup>32</sup>P-labelled full-length *POPTc80* ORF (open reading frame), washed twice with 2  $\times$  SSC (1  $\times$  SSC is 0.15 M NaCl/0.015 M sodium citrate)/0.1% SDS at 42 and 55°C for 15 min each and then washed with 0.1  $\times$  SSC/0.1% SDS at 65°C for 30 min before exposure to an X-ray film.

### POP Tc80 expression in *Escherichia coli*

A 2094 bp *POPTc80* ORF was amplified from TOPO-*POPTc80* using forward (5'-ccaacaCATATGCGCAGCGTTTACCCGTT-3'; lower-case, random bases; underlined, the NdeI site; boldface, initiation codon) and reverse (5'-ctatgaactcGAGTTACTCTTTCCACGAAGCATTG-3'; underlined, the XhoI site; boldface, stop codon) primers under the PCR conditions described above. The fragment produced was digested and cloned into the NdeI and XhoI sites of the pET-15b vector (Novagen, Carlsbad, CA, U.S.A.) and correct cloning in the desired orientation was confirmed by sequencing. The N-terminal His-tagged POP Tc80 was expressed in *E. coli* BL21 (DE3) by 0.5 mM IPTG (isopropylthio- $\beta$ -D-galactoside) induction at 16°C for 5 h. To purify the recombinant proteinase (rPOP Tc80), cells were harvested, lysed with Bugbuster<sup>™</sup> (Novagen) and centrifuged at 16000 g for 20 min at 4°C. The supernatant was submitted to affinity chromatography on a nickel-agarose resin (Sigma) at 4°C. After the resin had been extensively washed with a buffer containing 50 mM Na<sub>2</sub>HPO<sub>4</sub> (pH 8.0), 0.5 M NaCl and 20 mM imidazole, bound rPOP Tc80 was eluted with the same buffer containing 250 mM imidazole. The His tag was cleaved from the proteinase by biotinylated thrombin using the Thrombin Cleavage Capture Kit<sup>™</sup> (Novagen). Next, thrombin was eliminated from the reaction mixture by its adsorption on a streptavidin-agarose resin, whereas undigested proteins and free tags in the reaction mixture were further eliminated by nickel-agarose batch processing followed by dialysis against 25 mM Hepes (pH 7.5) and stored in 50% (v/v) glycerol at -20°C. The purified rPOP Tc80 and soluble proteins from BL21 bacteria either containing pET-15b/*POPTc80* plasmid or empty vector were subjected to SDS/PAGE (10% polyacrylamide) under reducing conditions followed by Coomassie Blue staining of the gel [15].

### Production of anti-rPOP Tc80 antibodies

Five male BALB/C mice were immunized with 5  $\mu$ g aliquots of purified rPOP Tc80 emulsified in complete Freund's adjuvant followed by four biweekly boosters with protein in incomplete Freund's adjuvant. Sera were collected after each booster for monitoring specific antibody production by Western blotting using *T. cruzi* epimastigote protein extract. At the end of 8 weeks, sera were collected, diluted 1:1 in glycerol (v/v) and stored at -20°C.

### Immunoblotting

Soluble protein extracts (20  $\mu$ g) from IPTG-induced BL21 bacteria either carrying *POPTc80* or empty vector, rPOP Tc80 (100 ng) or total proteins from amastigotes, epimastigotes or trypomastigotes of *T. cruzi*, corresponding to 5  $\times$  10<sup>6</sup> cells/well, were subjected to SDS/PAGE (10% polyacrylamide) under reducing conditions. Parasites were solubilized directly in the electrophoretic sample buffer. The proteins were transferred on to a nitrocellulose membrane and blocked by incubation in 5% (w/v) non-fat milk/PBS overnight at 4°C. Blots were incubated for 2 h with rPOP Tc80 antiserum, or purified POP Tc80 antiserum [5] or anti-tubulin monoclonal antibody (TAT-1) diluted in

1% non-fat milk/PBS. After four washes of 5 min each with PBS, membranes were incubated for 1 h with appropriate alkaline phosphatase-conjugated goat anti-IgG diluted to 1:5000, washed as above, and immunocomplexes were revealed with the alkaline-phosphatase substrate 5-bromo-4-chloro-3-indolyl-1-phosphate/Nitro Blue Tetrazolium (Sigma).

### Assay of enzyme activity

Recombinant POP Tc80 activity was determined by measuring the fluorescence of AMC (7-amido-4-methylcoumarin) released by hydrolysis of the enzyme substrate N-Suc-Gly-Pro-Leu-Gly-Pro-AMC [4], where Suc stands for succinyl. Purified rPOP Tc80 was assayed in reaction buffer [25 mM Hepes and 5 mM DTT (dithiothreitol), pH 7.5] containing 20  $\mu$ M substrate in 100  $\mu$ l final volume. The fluorescence of AMC released by the enzymatic reaction was recorded as described previously [5]. The rPOP Tc80 activity was also assayed using different peptides under the same experimental conditions (N-Boc-Val-Leu-Lys-AMC, N-Boc-Leu-Lys-Arg-AMC, N-Cbz-Val-Lys-Met-AMC, N-Boc-Leu-Gly-Arg-AMC, N-Boc-Ile-Gly-Gly-Arg-AMC, N-Suc-Leu-Tyr-AMC, N-Suc-Ala-Ala-Ala-AMC, N-Boc-Val-Pro-Arg-AMC, N-Suc-Gly-Pro-AMC, N-Cbz-Gly-Gly-Arg-AMC, N-Suc-Ala-Ala-Pro-Phe-AMC, N-Cbz-Phe-Arg-AMC, H-Gly-Arg-AMC, H-Gly-Phe-AMC, Ala-Ala-Phe-AMC, L-Arg-AMC and L-Ala-AMC and L-Lys-Ala-AMC, where Boc and Cbz stand for t-butoxycarbonyl and benzyloxycarbonyl respectively). To determine kinetic parameters, recombinant (0.67 ng) or native (0.26 ng) POP Tc80 was incubated in reaction buffer with variable N-Suc-Gly-Pro-Leu-Gly-Pro-AMC substrate concentrations (3.12–100  $\mu$ M) and the AMC release was measured as described above.  $K_m$  and  $V_{max}$  values were determined by hyperbolic regression using the method of Cornish-Bowden [16]. The  $k_{cat}$  was calculated using  $k_{cat} = V_{max}/[E]_0$ , where  $[E]_0$  represents the active enzyme concentration. Quantification of active rPOP Tc80 was performed by incubation of the protein with serial concentrations of the irreversible chloromethane POP Tc80 inhibitor as described in [5].

### Assay of rPOP Tc80 and *T. cruzi* host cell invasion inhibitions

Different concentrations (over the range 0.01–100 nM) of POP Tc80 inhibitors [17] were used to assay rPOP Tc80 inhibition. The values of inhibition coefficient  $K_i$  were determined as described in [5].

Trypomastigotes ( $5 \times 10^6$  cells/ml) were incubated for 1 h at 37°C in culture medium containing different concentrations of inhibitors and then transferred on to murine muscle L-6 cell culture, 24 h after plating, on sterile circular coverglasses in 24-well plates with a trypomastigote/host cell ratio of 20:1. After a 4 h incubation, cells were washed three times with culture medium and fixed overnight at 4°C in 3.7% (v/v) formaldehyde. After several washes with PBS, cells were incubated with 5% (w/v) non-fat milk in PBS for 30 min, followed by incubation with serum from a patient with chronic Chagas disease. Cells were washed several times and then incubated with FITC-conjugated goat anti-human IgG for 1 h. This was followed by secondary antibody removal before staining the host cell and parasite DNAs with 5  $\mu$ g/ml DAPI (4,6-diamidino-2-phenylindole) for 5 min. Coverslips were mounted in FluoroGuard antifade reagent (Bio-Rad Laboratories, Hercules, CA, U.S.A) and observed by epifluorescence microscopy. DAPI-positive parasites with a negative immunolabelling were counted as intracellular parasites, whereas parasites labelled with anti-*T. cruzi* antibodies were considered extracellular [5,10]. The number of internalized parasites in an L-6 cell was determined by observation of at least 500 cells.

### Homology molecular modelling of POP Tc80

Template structures used for POP Tc80 homology modelling were selected by searching the Brookhaven PDB (Protein Data Bank; <http://www.rcsb.org/pdb/>). The following structures were used to construct models of POP Tc80: POP chains A from porcine brain (PDB code 1H2W) and porcine muscle (PDB code 1QFM). Alignment of the selected templates to the POP Tc80 sequence was performed using Clustal W [18]. A preliminary three-dimensional model for both templates was first obtained using the InsightII homology module software (Accelrys; <http://www.accelrys.com/>) and Modeler [19]. Side chains were rebuilt and their structural positions were corrected based on a library of allowed side-chain rotamers. Finally, the overall model quality was verified by analysing the three-dimensional properties of each residue and the packing of the structure was checked. The final model structure was selected to be from the 1QFM template. In this way, its co-ordinates were refined by several rounds of energy minimization (1000 steps of steepest descents followed by conjugate gradients until convergence). The side-chain positions were first optimized, keeping the full backbone fixed. This constraint was then removed until the conjugate-gradient algorithm converged. The InsightII Discover module was used for that purpose with a distance-dependent dielectric constant and a cut-off of 20 Å (1 Å = 0.1 nm). No charged groups (N- and C-terminal groups, Asp, Glu, Arg and Lys side chains) were considered at this point to avoid unexpected ionic intramolecular interactions in vacuum. The consistent valence forcefield (CVFF) was used. The model quality was further assessed with the programs PROCHECK [20] and WHATIF [21].

The final step was to dock a triple-helical structure of collagen within the POP Tc80 model. For that purpose, we first checked the cavity size and volume of the POP Tc80 active-site model after the previous molecular dynamics runs, especially following the flux of water molecules into and out of the model. We therefore manually docked the triple-helical structure of collagen (integrin-binding collagen peptide with sequence (Gly-Pro-Hyp)<sub>2</sub>-Gly-Phe-Hyp-Gly-Glu-Arg-(Gly-Pro-Hyp) [22], in which each of the phenylalanine, glutamate and arginine residues was replaced by a glycine residue using these characteristics, positioning the collagen appropriate scissile bond in the vicinity of the POP Tc80 active-site residues Ser<sup>548</sup>, His<sup>667</sup> and Asp<sup>631</sup>. This preliminary model of the POP Tc80–collagen complex was first energy-refined by the conjugate gradient algorithm (10<sup>4</sup> iterations), considering the C $\alpha$  enzyme backbone atoms as fixed. Further rounds of small molecular dynamics runs (10 ps) followed by energy minimization (10<sup>4</sup> steps) were next performed to stabilize the system until energy convergence of the whole protein + ligand + water layer system.

## RESULTS

### Cloning and sequencing of POP cDNA from *T. cruzi*

The sequence of cloned POP Tc80 cDNA (2155 bp) contains 61 bp from the 5'-UTR and 2094 bp as the POP Tc80 ORF, which codes for a polypeptide of 697 amino acids with a calculated molecular mass of 78.230 kDa. The POP Tc80 cDNA did not contain any stop codon in its 5'-UTR region; thus the initiation codon was established as the first methionine residue after the miniexon sequence. This was based on a comparison of the deduced POP Tc80 sequence with POP sequences from *Homo sapiens*, *Sus scrofa*, *Aeromonas hydrophila* and *Dictyostelium discoideum*, which showed that residues tyrosine, proline and arginine close to the first methionine, i.e. MRSVYPLAR, are conserved in the N-terminal region of POPs in those organisms



Figure 1 Alignment of *T. cruzi* POP Tc80 with other POPs

Amino acid deduced sequences from *Trypanosoma cruzi* POP Tc80 (GenBank® accession no. AF452421), *Homo sapiens* POP (accession no. X74496 [51]), *Sus scrofa* (accession no. M64227 [52]), *Aeromonas hydrophila* POP (accession no. D14005 [53]), *Dictyostelium discoideum* POP (accession no. AJ238018 [54]) and *T. cruzi* oligopeptidase B (OP-Tc; accession no. U69897 [30]) were aligned using the CLUSTAL W program. Arrowheads indicate the catalytic triad.

(Figure 1). In addition, no signal peptide was predicted from the POP Tc80 sequence, although it is secreted by infective trypomastigote forms [4].

Amino acid sequence alignment confirmed that POP Tc80 belongs to the POP family of serine proteinases. POP Tc80 shared 43% identity with many mammalian POPs, such as porcine POP, whose molecular structure has been determined [9]. The level of identity of POP Tc80 was as high as 55% with POPs in general, when the region of interest was the C-terminal portion (starting from residue 430) that comprises the catalytic domain and is the most conserved region in this proteinase family (Figure 1). The POP Tc80 catalytic triad is composed of highly conserved

Ser<sup>548</sup>, Asp<sup>631</sup> and His<sup>667</sup> (Ser<sup>554</sup>, Asp<sup>641</sup> and His<sup>680</sup> in porcine POP). Moreover, the similarity of POP Tc80 to *T. cruzi* oligopeptidase B was weaker, with only 22% identity. This enzyme is also considered to be a member of the S9 family of serine proteinases, although it is not a true POP since it does not cleave after the proline residue [23].

#### Genomic organization and expression of the POP Tc80 gene

A single band was revealed by Southern blotting of *T. cruzi* genomic DNA digested with ClaI, EcoRV, HindIII or XhoI

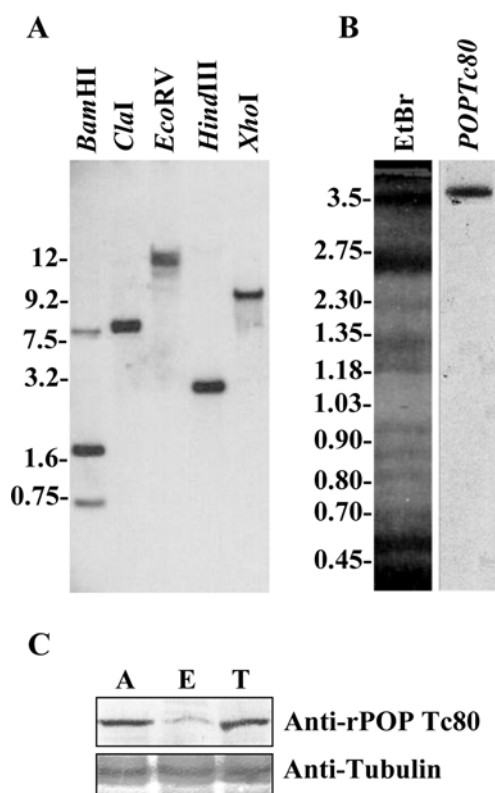


**Figure 2** Analyses of gene copy number, chromosome location and expression pattern of POP Tc80 in *T. cruzi*

(A) The *T. cruzi* genomic DNA was fragmented by BamHI, ClaI, EcoRV, HindIII or XhoI restriction enzymes, separated on 0.8% agarose gel, transferred on to a nylon membrane and probed with the radiolabelled full-length *POPTc80* ORF. The sizes of probed fragments (in kb) are indicated. (B) Chromosomal mapping of *POPTc80*. A pulsed-field gel of the clone CL-Brener was stained by ethidium bromide (left, chromosomal bands are shown in megabases), blotted on to a nylon membrane (right) and probed as described above. (C) POP Tc80 expression analysis in the different *T. cruzi* stages ( $5 \times 10^6$  cells/well) by Western blotting using rPOP Tc80 antiserum. Loading control was performed using anti-tubulin TAT-1 monoclonal antibody. A, amastigote stage; E, epimastigote stage; T, trypomastigote stage.

restriction enzymes and probed with the full-length POP Tc80 cDNA (Figure 2A). DNA digested with enzymes that present a single site on the POP Tc80 gene, such as EcoRI (results not shown), or two, such as BamHI (Figure 2A), generated two and three bands respectively. The probe readily hybridized with a 747 bp BamHI digest product, which is in agreement with the presence of sites at positions 342 and 1089 in *POPTc80*. These results suggest that the *POPTc80* gene is represented as a single copy per haploid genome. Consistent with this, Southern-blot analysis of chromosome DNA separated by pulsed-field gel electrophoresis revealed that *POPTc80* maps to a single chromosomal band of 3.5 Mb (Figure 2B).

To test the level of expression of POP Tc80 throughout the life cycle of *T. cruzi*, we use the anti-rPOP Tc80 antibody produced in mice to perform a Western blot of the three parasitic developmental stages. POP Tc80 is at least three times more abundant in trypomastigotes and amastigotes than in epimastigotes (Figure 2C). In this experiment, we used the same number of cells of each developmental stage. Thus, these results corroborate our previous investigation showing that epimastigotes display only 35% of the POP Tc80 enzymatic activity as that observed in trypomastigotes [4]. No labelling was observed with preimmune

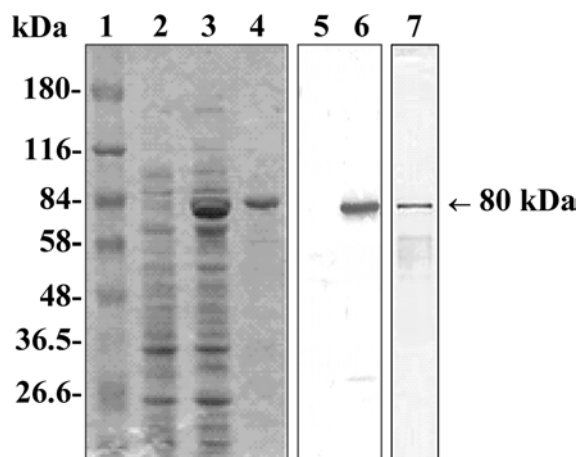


**Figure 3** Expression of recombinant POP Tc80

BL21 bacteria either containing pET-15b/*POPTc80* plasmid (lane 3) or empty vector (lane 2) were induced by 0.5 mM IPTG for 5 h at 16°C; the recombinant protein was purified by affinity chromatography on a nickel-agarose resin (lane 4) and analysed by SDS/PAGE (10% polyacrylamide) under reducing conditions and Coomassie Blue staining. Western blotting was performed as described in the Experimental section using anti-native POP Tc80 antibody (lane 5, extract from bacteria containing empty vector; lane 6, extract from bacteria containing pET-15b/*POPTc80*; lane 7, purified rPOP Tc80). Lane 1, molecular-mass standards.

sera (results not shown). These results show that POP Tc80 is differentially expressed in *T. cruzi* life cycle stages.

### Recombinant and native POP Tc80 display similar biochemical and kinetic properties

After induction by IPTG, a fresh soluble extract of BL21 bacteria containing pET-15b/*POPTc80* showed significant activity on N-Suc-Gly-Pro-Leu-Gly-Pro-AMC-specific POP Tc80 substrate, whereas extracts of bacteria transformed with empty vector did not (results not shown). Non-purified and purified rPOP Tc80 showed the same electrophoretic profile compared with the native enzyme, with an 80 kDa band on SDS/PAGE under reducing conditions after boiling (Figure 3, lanes 3 and 4). The authenticity of rPOP Tc80 expression was confirmed by Western-blot analysis of these extracts using native POP Tc80-specific antiserum. A single band of the expected size was revealed only from *E. coli* extracts containing the recombinant plasmid carrying the *POPTc80* as well as the affinity-purified rPOP Tc80 (Figure 3, lanes 6 and 7).

Enzymatic assays performed to determine the effect of compounds such as salt, detergent and reducing agents on rPOP Tc80 showed that reducing agents such as DTT and 2-mercaptoethanol significantly increased its activity. The catalytic efficiency of the enzyme was 14-fold higher in the presence of DTT than in its absence (results not shown). This effect has been observed for *T. brucei* oligopeptidase B, in which maximal activity was recorded with 10 mM DTT [23]. Therefore enzymatic assays were performed in the presence of 5 mM DTT.

The recombinant POP Tc80 presented kinetic properties approximating those obtained for the native enzyme, using N-Suc-Gly-Pro-Leu-Gly-Pro-AMC (Table 1). To evaluate whether rPOP Tc80 could effectively hydrolyse substrates other than N-Suc-Gly-Pro-Leu-Gly-Pro-AMC, we assayed its activity on several fluorogenic substrates. Only substrates containing proline residues in the P<sub>1</sub> position, such as N-Suc-Gly-Pro-AMC, were cleaved (24% of the activity obtained using N-Suc-Gly-Pro-Leu-Gly-Pro-AMC), with the exception of N-Suc-Ala-Ala-Ala-AMC.

**Table 1 Kinetic properties of recombinant and native POP Tc80 using N-Suc-Gly-Pro-Leu-Gly-Pro-AMC substrate**

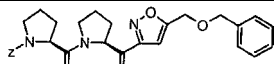
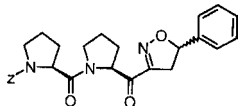
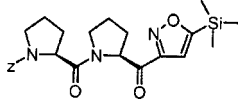
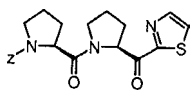
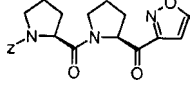
POP Tc80	$K_m$ ( $\mu\text{M}$ )	$k_{\text{cat}}$ ( $\text{s}^{-1}$ )†	$k_{\text{cat}}/K_m$ ( $\mu\text{M}^{-1} \cdot \text{s}^{-1}$ )
Recombinant*	18.1	48.7	2.68
Native	14.0	28.1	2.00

\* Reactions were performed using the purified His-tag-free rPOP Tc80.

†  $k_{\text{cat}}$  values were calculated assuming the molecular mass of the POP Tc80 to be 78.230 kDa.

**Table 2 Inhibition of recombinant and native POP Tc80**

Z, benzyloxycarbonyl.

Compound*	$K_i$ (nM)†	
	Recombinant	Native‡
1 	0.80	0.28
2 	0.48	0.21
3 	1.52	0.45
4 	0.90	0.26
5 	83	72

\* Inhibitors were developed for native POP Tc80 by Bal et al. [17].

† Enzyme inhibition was measured in triplicate using N-Suc-Gly-Pro-Leu-Gly-Pro-AMC.

‡ From [17].

This last substrate showed a weaker ratio of hydrolysis with no more than 13% of that obtained for N-Suc-Gly-Pro-Leu-Gly-Pro-AMC. The activities of POPs towards alanine residues in the  $P_1$  position have been described in [24]. An example is the porcine muscle POP that cleaves mastoporan, a bioactive peptide (Ile-Asn-Leu-Lys-Ala-Leu-Ala-Ala-Leu-Ala-Lys-Ile-Leu-NH<sub>2</sub>), after all alanine residues [25]. No hydrolysis was recorded for the other substrates tested containing lysine, arginine, methionine, tyrosine or phenylalanine in the  $P_1$  position. Furthermore, rPOP Tc80 was capable of hydrolysing both purified and native type I collagen (results not shown) with features comparable with those displayed by its native form [4].

### Recombinant and native POP Tc80 show similar sensitivities to inhibitors

POP inhibitors [17] were assayed on recombinant POP Tc80 activity. Table 2 shows the inhibitory effects of some of these inhibitors on the recombinant and native POP Tc80 towards the fluorogenic substrate N-Suc-Gly-Pro-Leu-Gly-Pro-AMC. Both

enzymes were highly inhibited by compounds 1–4 with  $K_i$  values over the range 0.26–1.52 nM. In contrast, their activities were less sensitive to compound 5. These results indicate that recombinant and native POP Tc80 show similar inhibition profiles.

### Inhibition of the host cell invasion by POP Tc80 inhibitors results from the inhibition of the entry process itself rather than from the inhibition of parasite attachment to host cells

We previously showed that POP Tc80 inhibitors blocked non-phagocytic cell invasion by trypomastigotes [5]. Host cell invasion is a complex process that can be divided into two major steps: (i) parasite attachment to the host cell through protein binding to extracellular matrix components or cell-surface carbohydrates; (ii) parasite internalization involving early signal transduction events that lead to the recruitment and fusion of host lysosomes at the parasite attachment site. To distinguish the involvement of POP Tc80 in these two steps, we tested the effects of specific POP Tc80 inhibitors on host cell invasion by trypomastigotes, using a parasite in-out immunostaining technique that allows us to distinguish internalized parasites from those attached to the host cell. Figure 4 shows the inhibitory effects of compounds 1, 2 and 4. Taking into account the number of intracellular parasites per cell, parasite invasion was precluded by compounds 1 and 2 with IC<sub>50</sub> values of approx. 10  $\mu\text{M}$  and, to a lesser extent, by compound 4 (Figure 4B). When taking into account the number of attached parasites per cell, an inverse relation was observed between the increase in the number of parasites attached to host cells and the increase in drug concentration (Figure 4A). Under the conditions used in this experiment, these inhibitors were toxic neither to host cells nor to trypomastigotes (results not shown). These results strongly suggest that POP Tc80 inhibitors act through the inhibition of the invasion itself of host cells rather than through the inhibition of trypomastigote attachment to the host cell surface.

### Molecular modelling of POP Tc80

To construct a three-dimensional molecular model of POP Tc80, we used the molecular structure of the crystallized porcine POP as a template [9]. These proteins share 43% amino acid identity (Figure 1), allowing the prediction of the model. Two characteristic domains of POPs constitute the POP Tc80 architecture, which are superimposable on those of the porcine POP (Figures 5A and 5B). The catalytic domain exhibits a characteristic  $\alpha/\beta$ -hydrolase fold [26] composed of residues 1–74 and 435–697. The core domain contains a central  $\beta$ -sheet, composed of eight strands, of which only one is antiparallel. Five helices surround the central  $\beta$ -sheets. The active site consists of Ser<sup>548</sup> as the nucleophile and His<sup>667</sup> as the proton carrier, whereas Asp<sup>631</sup> maintains the imidazole ring in a suitable position for capturing the serine proton during catalysis. Ser<sup>548</sup> is a part of the conserved GGSNGG sequence among POPs and is situated at the 'nucleophilic elbow' between a strand and a helix [26]. The catalytic triad is located in the interface between  $\alpha/\beta$ -hydrolase and the non-catalytic domain and is accessible from the large pocket.

The second domain is folded from residues 75–425 forming the non-catalytic domain. This portion is composed of a set of seven similar  $\beta$ -sheets that collectively form a  $\beta$ -propeller structure. Four antiparallel  $\beta$ -strands correspond to a blade of the propeller and the series of blades are twisted and radially positioned around a central axis forming a central cavity as a funnel (Figures 5C and 5D). This three-dimensional arrangement provides a flattened structure having a lower face with the funnel opening towards the external milieu and an upper face of the propeller domain,

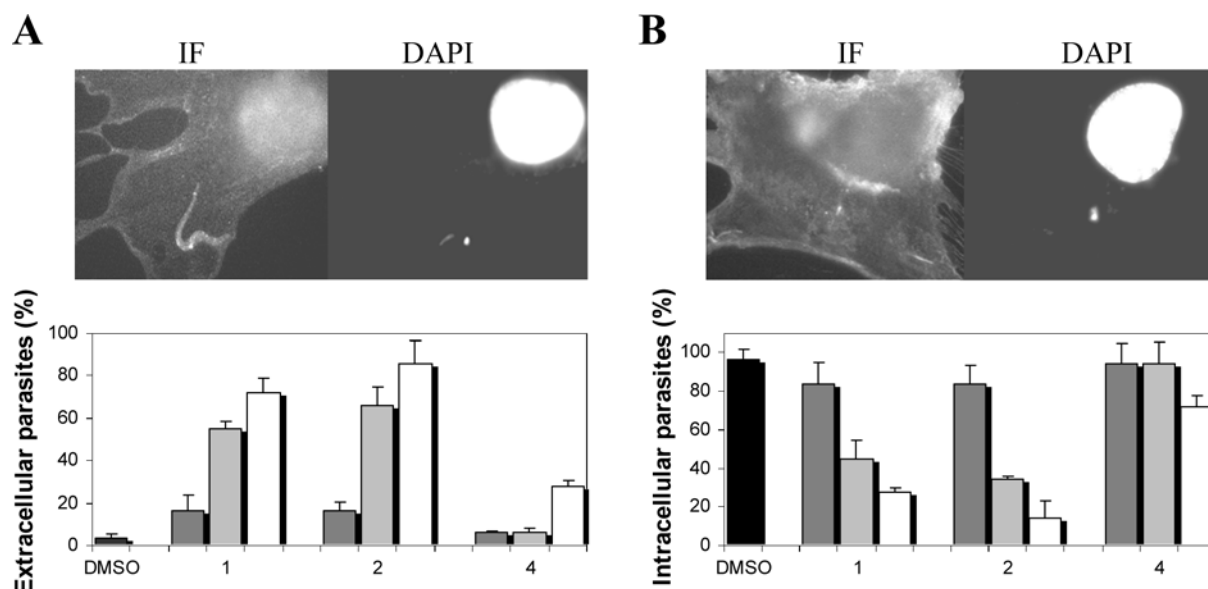


**Figure 4** POP Tc80 inhibitors block trypanomastigote's entry into host cells but not attachment to their surface

Trypomastigotes were preincubated for 1 h with 10  $\mu\text{M}$  (dark grey), 25  $\mu\text{M}$  (light grey) and 100  $\mu\text{M}$  (white) of inhibitors 1, 2 and 4, transferred on to murine muscle L-6 cell cultures. After a 4 h incubation, the cells were washed, fixed with formaldehyde and subjected to immunofluorescence (IF) assay and DAPI staining to distinguish the parasites attached to the host cell (A, extracellular parasites) from those internalized (B, intracellular parasites). Values on ordinates represent number of parasites/100 L6 cells. Controls (black) consisted of parasites maintained without inhibitor and with the same concentrations of DMSO. Each value is the mean  $\pm$  S.D. for triplicate experiments.

covalently joined to the  $\alpha/\beta$ -hydrolase domain. As in porcine POP, the first and the seventh blades of POP Tc80  $\beta$ -propeller are not linked by either disulphide or covalent bonds, unlike other known  $\beta$ -propeller structures [27,28], but only by hydrophobic interactions and salt bridges that render POP Tc80  $\beta$ -propeller a flexible domain.

We performed docking calculations to determine the interaction energies of the substrate-catalytic pocket, between the three-dimensional structure of triple-helical collagen and the proposed model of POP Tc80 structure. After the molecular dynamics/minimization rounds, it appears that the collagen would access the active site of POP Tc80 by the interface region located between the two domains ( $\alpha/\beta$ -hydrolase and  $\beta$ -propeller; Figure 6), facing the catalytic pocket, and not by the central pore formed on  $\beta$ -propeller structure [9]. Probably, by placing the collagen near the active site, its cleavage is facilitated by a move away from the peptidase and the propeller domains supported by a 'hinge' formed by the 1 and 7 blades that connects the two domains [29] (see the supplementary Figure at <http://www.BiochemJ.org/bj/388/bj3880029add.htm>). The root mean square deviation between the protein backbone atoms of the two complexes was 2.1 Å, revealing that the overall POP Tc80 structure was not modified by the inclusion of a large molecular system such as the collagen triple helix.

## DISCUSSION

Our previous studies have demonstrated that the secreted *T. cruzi* 80 kDa proteinase (initially named Tc80; [4]), an enzyme that displays collagenase-like activity, is a member of the POP family of serine proteinases [5]. In the present study, we cloned and sequenced the POP Tc80 gene whose deduced amino acid sequence analysis confirmed that it encodes a POP of *T. cruzi*. Since POP Tc80 is the first described protozoan POP, its closest homologous enzymes are related to mammalian POPs, sharing up to 44% identity. In contrast, trypanosomatid oligopeptidase B [23,30],

non-post-proline cleaving enzymes considered to be members of the S9 POP family, share 22% identity with POP Tc80.

No typical signal peptide was predicted for the deduced amino acid sequence of POP Tc80 regardless of the fact that the enzyme is both located inside vesicles and secreted by *T. cruzi* trypanomastigotes [4,5]. In this regard, several secreted proteins lacking typical signal peptides have been described in *Plasmodium falciparum*, such as GPB 130, RESA, FIRA and PfEMP1 [31–34]. Moreover, the inhibitor-2 of plasminogen activator that also has no typical signal peptide is probably secreted by means of hydrophobic amino acids located far from the N-terminal end [35]. Other reports have provided evidence for a post-translational protein translocation across the endoplasmic reticulum membrane that neither requires a typical N-terminal signal sequence nor involves the signal recognition particle. Instead, it requires a class of 70 kDa heat-shock proteins, which most probably play a role in the exposure of the hydrophobic core of proteins [36].

We have suggested that POP Tc80 could play a role in the invasion process of host cells by *T. cruzi*. This is supported by its secretion mainly by trypanomastigotes, the infective *T. cruzi* forms and POP Tc80-specific inhibitors that impair the entry of trypanomastigotes into mammalian host cells in a selective manner [4]. In the present study, we report other details that reinforce our initial proposition: (i) *T. cruzi* shows a significant increase in POP Tc80 expression during its trypanomastigote life cycle stage compared with its non-infective epimastigote stage, corroborating previous results that showed that trypanomastigotes display three times higher enzymatic activity compared with epimastigotes; and (ii) inhibition of host cell invasion by POP Tc80 inhibitors seems to be due to an inhibition of the entry process itself, rather than due to an inhibition resulting from trypanomastigote attachment to the host cell surface.

Recombinant POP Tc80 showed similar kinetic parameters and sensitivity to inhibitors compared with the native protein, indicating that it was correctly folded and preserved the biochemical features of its native form. Moreover, POP Tc80 apparently

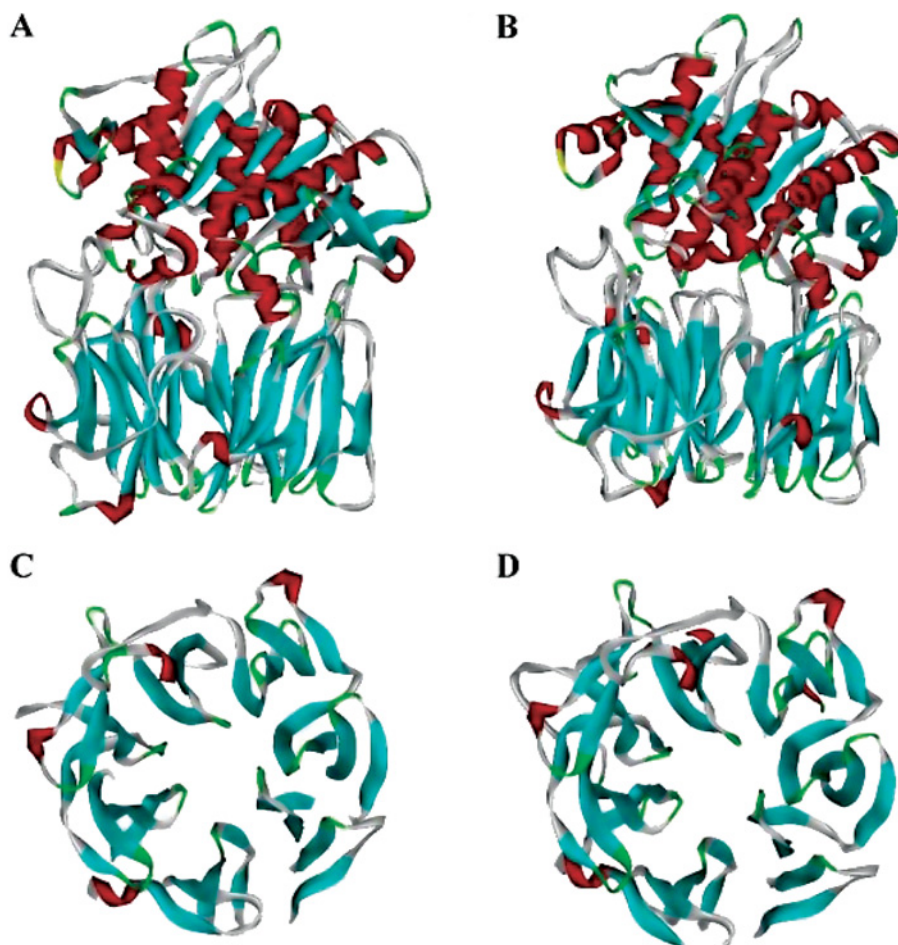


**Figure 5** Theoretical model of POP Tc80

The POP Tc80 model (A) is based on the crystallographic structure of porcine POP (B). The catalytic domain is composed of ten  $\alpha$ -helices (red) and ten  $\beta$ -strands (cyan) forming an  $\alpha/\beta$ -hydrolase-like structure. Yellow and green indicate turns. The non-catalytic  $\beta$ -propeller domain is located just below the catalytic domain and is composed of only antiparallel  $\beta$ -strands (cyan). The  $\beta$ -propeller domain of POP Tc80 (C) and porcine POP (D) is viewed perpendicular to that shown in (A, B). The  $\beta$ -sheets of the seven blades are joined in succession around the central axis.

does not undergo further post-translational modification since the bacterial intracellular environment is unfavourable for this. If it does, it is not required for its activity. We observed that DTT increased POP Tc80 catalytic efficiency on N-Suc-Gly-Pro-Leu-Gly-Pro-AMC. The oxidation of some cysteine residues could provide disulphide bridges, which make the POP Tc80 structure less flexible. This could impede access of the substrate to the catalytic pocket. It is known that POPs, including POP Tc80, are strongly inhibited by bulky reagents with specificity for cysteine residues [4,37]. This inhibition is certainly due to the Cys<sup>255</sup> situated close to the catalytic site in the folded enzyme [9], since POP from *Flavobacterium meningosepticum* has Cys<sup>255</sup> replaced by a threonine residue and is not inactivated by thiol inhibitors [38]. In this way, DTT could spare Cys<sup>255</sup> from injury.

The knowledge concerning the catalytic mechanism and architecture of the catalytic pocket of enzymes is very useful for improving the design of selective and specific inhibitors. To obtain some information about its catalytic and structural properties, we performed theoretical three-dimensional modelling of POP Tc80 based on the crystallized structure of porcine POP. We observed that residues comprising the catalytic triad of POP Tc80 and porcine POP are superimposed; however, the lateral chains of these residues are positioned at different angles (results not shown). Perhaps, these differences could change the stereospecificity for

substrates and thus for the inhibitors, as observed with those of POP Tc80 that block the activity of mammalian POPs with less efficiency [5,17,39]. Among the catalytic divergences reported, the main and the most intriguing is the ability of POP Tc80 to cleave triple-helical collagen fibres, in contrast with other POPs that are limited to hydrolysing small peptides. However, POP Tc80 is not the only POP member described with the capacity to degrade large polypeptides. Like POP Tc80, FAP $\alpha$  (fibroblast activation protein  $\alpha$  [40]), a dipeptidyl peptidase IV-like enzyme, readily degrades extracellular matrix collagens. FAP $\alpha$  is a type II membrane-bound glycoprotein expressed mainly in reactive tumour stromal fibroblasts and its collagenolytic activity contributes to remodelling and invasion of epithelial tumours. Moreover, it was reported recently that *Salmonella enterica* oligopeptidase B cleaves histones H2A and H4 *in vitro* [41] and that cytosolic prolyl endopeptidase is involved in the degradation of the p40-phox variant protein in myeloid cells [42]. It is interesting to note that, although POPs, FAP and oligopeptidase B, present quite divergent amino acid sequences, they share similar three-dimensional structures composed of  $\alpha/\beta$  hydrolase and  $\beta$ -propeller domains [43,44].

On the basis of our docking analysis, we suggest that access of the triple-helical collagen to the catalytic pocket of POP Tc80 takes place in the vicinity of the  $\alpha/\beta$  hydrolase and  $\beta$ -propeller

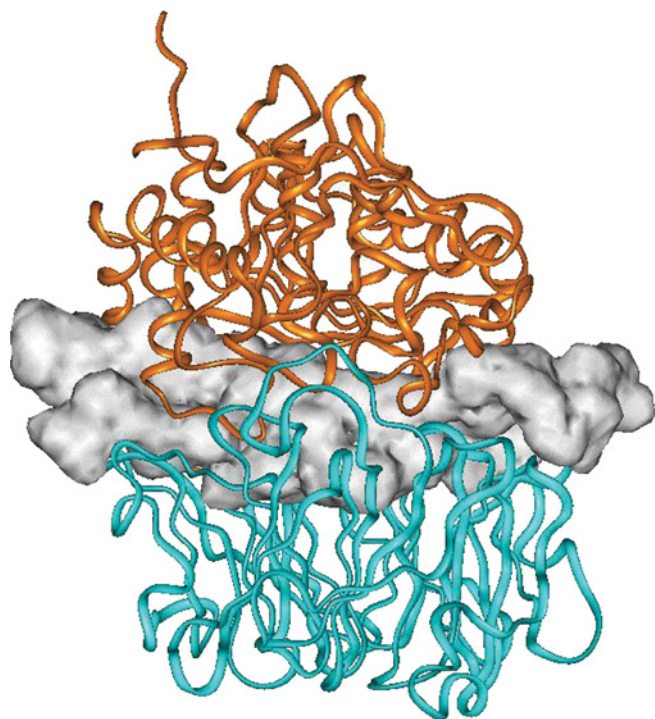


**Figure 6** Docking of triple-helical collagen with POP Tc80

The collagen (grey) interacts in the vicinity of the  $\alpha/\beta$ -hydrolase (orange C $\alpha$  trace ribbon) and  $\beta$ -propeller (cyan C $\alpha$  trace ribbon) domains.

interface. A comparable supposition has been reported by Rasmussen et al. [45], suggesting that the substrate entrance to the active site of dipeptidyl peptidase IV is probably through a side opening situated between a peptidase and  $\beta$ -propeller domains, which is the shortest and the most favourable accessible way to the catalytic pocket. A similar hypothesis has been experimentally validated in porcine POP by site-specific mutagenesis, where a disulphide bond between a peptidase and  $\beta$ -propeller domains prevents the access of the substrate towards the catalytic pocket [29]. Probably,  $\beta$ -propeller is the domain responsible for POP Tc80 and collagen interactions as already suggested for dipeptidyl peptidase IV and FAP $\alpha$  [46,47]. Moreover,  $\beta$ -propeller structures including the four-blade  $\beta$ -propeller of matrix metalloproteinase collagenases [48] are involved in multiple protein–protein interactions [49]. It has been shown that, although the  $\beta$ -propeller is not a catalytic domain, it is essential for the cleavage of collagen by matrix metalloproteinases [50].

We thank D. Engman, C. Deregnacourt and S. Freitas for a critical reading of this paper, A. Haemers for providing inhibitors, S. Charneau for producing anti-rPOP Tc80 antiserum, and Ana de Cássia Vexenat for technical support. This work was supported by CNPq (Conselho Nacional de Desenvolvimento Científico e Tecnológico) and CAPES, Brazil, and by CNRS (grants GDR 1077 and IFR 63) and MENRT (PRFMMIP) of France.

## REFERENCES

- Moncayo, A. (1999) Progress towards interruption of transmission of Chagas disease. *Mem. Inst. Oswaldo Cruz* **94**, 401–404
- Giordano, R., Fouts, D. L., Tewari, D., Colli, W., Manning, J. E. and Alves, M. J. (1999) Cloning of a surface membrane glycoprotein specific for the infective form of *Trypanosoma cruzi* having adhesive properties to laminin. *J. Biol. Chem.* **274**, 3461–3468
- Ortega-Barria, E. and Pereira, M. E. (1992) Entry of *Trypanosoma cruzi* into eukaryotic cells. *Infect. Agents Dis.* **1**, 136–145
- Santana, J. M., Grellier, P., Schrevel, J. and Teixeira, A. R. (1997) A *Trypanosoma cruzi*-secreted 80 kDa proteinase with specificity for human collagen types I and IV. *Biochem. J.* **325**, 129–137
- Grellier, P., Vendeville, S., Joyeau, R., Bastos, I. M., Drobecq, H., Frappier, F., Teixeira, A. R., Schrével, J., Davioud-Charvet, E., Sergheraert, C. et al. (2001) *Trypanosoma cruzi* prolyl oligopeptidase Tc80 is involved in nonphagocytic mammalian cell invasion by trypomastigotes. *J. Biol. Chem.* **276**, 47078–47086
- Vendeville, S., Buisine, E., Williard, X., Schrével, J., Grellier, P., Santana, J. and Sergheraert, C. (1999) Identification of inhibitors of an 80 kDa protease from *Trypanosoma cruzi* through the screening of a combinatorial peptide library. *Chem. Pharm. Bull. (Tokyo)* **47**, 194–198
- Joyeau, R., Maoulida, C., Guillet, C., Frappier, F., Teixeira, A. R., Schrével, J., Santana, J. and Grellier, P. (2000) Synthesis and activity of pyrrolidinyl- and thiazolidinyl-dipeptide derivatives as inhibitors of the Tc80 prolyl oligopeptidase from *Trypanosoma cruzi*. *Eur. J. Med. Chem.* **35**, 257–266
- Barrett, A. J. and Rawlings, N. D. (1992) Oligopeptidases, and the emergence of the prolyl oligopeptidase family. *Biol. Chem. Hoppe Seyler* **373**, 353–360
- Fulop, V., Bocskai, Z. and Polgar, L. (1998) Prolyl oligopeptidase: an unusual beta-propeller domain regulates proteolysis. *Cell (Cambridge, Mass.)* **94**, 161–170
- Tardieux, I., Webster, P., Ravesloot, J., Boron, W., Lunn, J. A., Heuser, J. E. and Andrews, N. W. (1992) Lysosome recruitment and fusion are early events required for trypanosome invasion of mammalian cells. *Cell (Cambridge, Mass.)* **71**, 1117–1130
- Ley, V., Robbins, E. S., Nussenzweig, V. and Andrews, N. W. (1990) The exit of *Trypanosoma cruzi* from the phagosome is inhibited by raising the pH of acidic compartments. *J. Exp. Med.* **171**, 401–413
- Milhausen, M., Nelson, R. G., Sather, S., Selkirk, M. and Agabian, N. (1984) Identification of a small RNA containing the trypanosome spliced leader: a donor of shared 5' sequences of trypanosomatid mRNAs? *Cell (Cambridge, Mass.)* **38**, 721–729
- Medina-Acosta, E. and Cross, G. A. (1993) Rapid isolation of DNA from trypanosomatid protozoa using a simple 'mini-prep' procedure. *Mol. Biochem. Parasitol.* **59**, 327–329
- Cano, M. I., Gruber, A., Vazquez, M., Cortes, A., Levin, M. J., Gonzalez, A., Degraeve, W., Rondinelli, E., Zingales, B., Ramirez, J. L. et al. (1995) Molecular karyotype of clone CL Brener chosen for the *Trypanosoma cruzi* genome project. *Mol. Biochem. Parasitol.* **71**, 273–278
- Laemmli, U. K. (1970) Cleavage of structural proteins during the assembly of the head of bacteriophage T4. *Nature (London)* **227**, 680–685
- Cornish-Bowden, A. (1976) *Principles of Enzyme Kinetics*, Butterworths, London
- Bal, G., Van der Veken, P., Antonov, D., Lambeir, A. M., Grellier, P., Croft, S. L., Augustyns, K. and Haemers, A. (2003) Prolylisoxazolones: potent inhibitors of prolyl oligopeptidase with antitrypanosomal activity. *Bioorg. Med. Chem. Lett.* **13**, 2875–2878
- Thompson, J. D., Higgins, D. G. and Gibson, T. J. (1994) CLUSTAL W: improving the sensitivity of progressive multiple sequence alignment through sequence weighting, position-specific gap penalties and weight matrix choice. *Nucleic Acids Res.* **22**, 4673–4680
- Marti-Renom, M. A., Stuart, A. C., Fiser, A., Sanchez, R., Melo, F. and Sali, A. (2000) Comparative protein structure modeling of genes and genomes. *Annu. Rev. Biophys. Biomol. Struct.* **29**, 291–325
- Laskowski, R. A., MacArthur, M. W., Moss, D. S. and Thornton, J. M. (1993) A program to check the stereochemical quality of protein structures. *J. Appl. Crystallogr.* **26**, 283–291
- Hooft, R. W., Vriend, G., Sander, C. and Abola, E. E. (1996) Errors in protein structures. *Nature (London)* **381**, 272
- Emsley, J., Knight, C. G., Farnside, R. W. and Barnes, M. J. (2004) Structure of the integrin  $\alpha 2 \beta 1$ -binding collagen peptide. *J. Mol. Biol.* **335**, 1019–1028
- Morty, R. E., Lonsdale-Eccles, J. D., Morehead, J., Caler, E. V., Mentele, R., Auerwald, E. A., Coetzer, T. H., Andrews, N. W. and Burleigh, B. A. (1999) Oligopeptidase B from *Trypanosoma brucei*, a new member of an emerging subgroup of serine oligopeptidases. *J. Biol. Chem.* **274**, 26149–26156
- Yoshimoto, T., Fischl, M., Orłowski, R. C. and Walter, R. (1978) Post-proline cleaving enzyme and post-proline dipeptidyl aminopeptidase. Comparison of two peptidases with high specificity for proline residues. *J. Biol. Chem.* **253**, 3708–3716
- Moriyama, A., Nakanishi, M. and Sasaki, M. (1988) Porcine muscle prolyl endopeptidase and its endogenous substrates. *J. Biochem. (Tokyo)* **104**, 112–117
- Óllis, D. L., Cheah, E., Cygler, M., Dijkstra, B., Frolow, F., Franken, S. M., Harel, M., Remington, S. J., Silman, I. and Schrag, J. (1992) The  $\alpha/\beta$  hydrolase fold. *Protein. Eng.* **5**, 197–211
- Li, J., Brick, P., O'Hare, M. C., Skarzynski, T., Lloyd, L. F., Curry, V. A., Clark, I. M., Bigg, H. F., Hazleman, B. L., Cawston, T. E. et al. (1995) Structure of full-length porcine synovial collagenase reveals a C-terminal domain containing a calcium-linked, four-bladed  $\beta$ -propeller. *Structure* **3**, 541–549

- 28 Baker, S. C., Saunders, N. F., Willis, A. C., Ferguson, S. J., Hajdu, J. and Fulop, V. (1997) Cytochrome cd1 structure: unusual haem environments in a nitrite reductase and analysis of factors contributing to beta-propeller folds. *J. Mol. Biol.* **269**, 440–455
- 29 Szeltner, Z., Rea, D., Juhasz, T., Renner, V., Fulop, V. and Polgar, L. (2004) Concerted structural changes in the peptidase and the propeller domains of prolyl oligopeptidase are required for substrate binding. *J. Mol. Biol.* **340**, 627–637
- 30 Burleigh, B. A., Caler, E. V., Webster, P. and Andrews, N. W. (1997) A cytosolic serine endopeptidase from *Trypanosoma cruzi* is required for the generation of Ca<sup>2+</sup> signaling in mammalian cells. *J. Cell Biol.* **136**, 609–620
- 31 Kochan, J., Perkins, M. and Ravetch, J. V. (1986) A tandemly repeated sequence determines the binding domain for an erythrocyte receptor binding protein of *P. falciparum*. *Cell* (Cambridge, Mass.) **44**, 689–696
- 32 Favaloro, J. M., Coppel, R. L., Corcoran, L. M., Foote, S. J., Brown, G. V., Anders, R. F. and Kemp, D. J. (1986) Structure of the RESA gene of *Plasmodium falciparum*. *Nucleic Acids Res.* **14**, 8265–8277
- 33 Lingelbach, K. R. (1993) *Plasmodium falciparum*: a molecular view of protein transport from the parasite into the host erythrocyte. *Exp. Parasitol.* **76**, 318–327
- 34 Baruch, D. I., Pasloske, B. L., Singh, H. B., Bi, X., Ma, X. C., Feldman, M., Taraschi, T. F. and Howard, R. J. (1995) Cloning the *P. falciparum* gene encoding PfEMP1, a malarial variant antigen and adherence receptor on the surface of parasitized human erythrocytes. *Cell* (Cambridge, Mass.) **82**, 77–87
- 35 Ye, R. D., Wun, T. C. and Sadler, J. E. (1988) Mammalian protein secretion without signal peptide removal. Biosynthesis of plasminogen activator inhibitor-2 in U-937 cells. *J. Biol. Chem.* **263**, 4869–4875
- 36 Brodsky, J. L. (1996) Post-translational protein translocation: not all hsc70s are created equal. *Trends Biochem. Sci.* **21**, 122–126
- 37 Knisatschek, H. and Bauer, K. (1979) Characterization of 'thyrolyberin-deamidating enzyme' as a post-proline-cleaving enzyme. Partial purification and enzyme-chemical analysis of the enzyme from anterior pituitary tissue. *J. Biol. Chem.* **254**, 10936–10943
- 38 Yoshimoto, T., Walter, R. and Tsuru, D. (1980) Proline-specific endopeptidase from *Flavobacterium*. Purification and properties. *J. Biol. Chem.* **255**, 4786–4792
- 39 Vendeville, S., Goossens, F., Debrey-Fontaine, M. A., Landry, V., Davioud-Charvet, E., Grellier, P., Scharpe, S. and Sergheraert, C. (2002) Comparison of the inhibition of human and *Trypanosoma cruzi* prolyl endopeptidases. *Bioorg. Med. Chem.* **10**, 1719–1729
- 40 Park, J. E., Lenter, M. C., Zimmermann, R. N., Garin-Chesa, P., Old, L. J. and Rettig, W. J. (1999) Fibroblast activation protein, a dual specificity serine protease expressed in reactive human tumor stromal fibroblasts. *J. Biol. Chem.* **274**, 36505–36512
- 41 Morty, R. E., Fulop, V. and Andrews, N. W. (2002) Substrate recognition properties of oligopeptidase B from *Salmonella enterica* serovar Typhimurium. *J. Bacteriol.* **184**, 3329–3337
- 42 Hasebe, T., Hua, J., Someya, A., Morain, P., Checler, F. and Nagaoka, I. (2001) Involvement of cytosolic prolyl endopeptidase in degradation of p40-phox splice variant protein in myeloid cells. *J. Leukoc. Biol.* **69**, 963–968
- 43 Gerczei, T., Keseru, G. M. and Naray-Szabo, G. (2000) Construction of a 3D model of oligopeptidase B, a potential processing enzyme in prokaryotes. *J. Mol. Graph. Model.* **18**, 7–17, 57–58
- 44 Ajami, K., Abbott, C. A., Obradovic, M., Gysbers, V., Kahne, T., McCaughan, G. W. and Gorrell, M. D. (2003) Structural requirements for catalysis, expression, and dimerization in the CD26/DPIV gene family. *Biochemistry* **42**, 694–701
- 45 Rasmussen, H. B., Branner, S., Wiberg, F. C. and Wagtmann, N. (2003) Crystal structure of human dipeptidyl peptidase IV/CD26 in complex with a substrate analog. *Nat. Struct. Biol.* **10**, 19–25
- 46 Cheng, H. C., Abdel-Ghany, M., Elble, R. C. and Pauli, B. U. (1998) Lung endothelial dipeptidyl peptidase IV promotes adhesion and metastasis of rat breast cancer cells via tumor cell surface-associated fibronectin. *J. Biol. Chem.* **273**, 24207–24215
- 47 Loster, K., Zeilinger, K., Schuppan, D. and Reutter, W. (1995) The cysteine-rich region of dipeptidyl peptidase IV (CD 26) is the collagen-binding site. *Biochem. Biophys. Res. Commun.* **217**, 341–348
- 48 Li, J., Brick, P., O'Hare, M. C., Skarzynski, T., Lloyd, L. F., Curry, V. A., Clark, I. M., Bigg, H. F., Hazleman, B. L. and Cawston, T. E. (1995) Structure of full-length porcine synovial collagenase reveals a C-terminal domain containing a calcium-linked, four-bladed beta-propeller. *Structure* **3**, 541–549
- 49 Adams, J., Kelso, R. and Cooley, L. (2000) The kelch repeat superfamily of proteins: propellers of cell function. *Trends Cell Biol.* **10**, 17–24
- 50 Bode, W. (1995) A helping hand for collagenases: the haemopexin-like domain. *Structure* **3**, 527–530
- 51 Vanhoof, G., Goossens, F., Hendriks, L., De Meester, I., Hendriks, D., Vriend, G., Van Broeckhoven, C. and Scharpe, S. (1994) Cloning and sequence analysis of the gene encoding human lymphocyte prolyl endopeptidase. *Gene* **149**, 363–366
- 52 Rennex, D., Hemmings, B. A., Hofsteenge, J. and Stone, S. R. (1991) cDNA cloning of porcine brain prolyl endopeptidase and identification of the active-site seryl residue. *Biochemistry* **30**, 2195–2203
- 53 Kanatani, A., Yoshimoto, T., Kitazono, A., Kokubo, T. and Tsuru, D. (1993) Prolyl endopeptidase from *Aeromonas hydrophila*: cloning, sequencing, and expression of the enzyme gene, and characterization of the expressed enzyme. *J. Biochem. (Tokyo)* **113**, 790–796
- 54 Williams, R. S., Eames, M., Ryves, W. J., Viggars, J. and Harwood, A. J. (1999) Loss of a prolyl oligopeptidase confers resistance to lithium by elevation of inositol (1,4,5) trisphosphate. *EMBO J.* **18**, 2734–2745

Received 21 June 2004/29 November 2004; accepted 7 December 2004

Published as BJ Immediate Publication 7 December 2004, DOI 10.1042/BJ20041049